Directive and focused acoustic wave radiation by tessellated transducers with folded curvatures

Danielle T. Lynd, Chengzhe Zou, Joseph Crump, and Ryan L. Harne

Citation: Proc. Mtgs. Acoust. **30**, 055010 (2017); doi: 10.1121/2.0000667
View online: https://doi.org/10.1121/2.0000667
View Table of Contents: http://asa.scitation.org/toc/pma/30/1
Published by the Acoustical Society of America

Proceedings of Meetings on Acoustics

Volume 30 http://acousticalsociety.org/

Acoustics `17 Boston

173rd Meeting of Acoustical Society of America and 8th Forum Acusticum
Boston, Massachusetts
25-29 June 2017

Signal Processing in Acoustics: Paper 2pSP6

Directive and focused acoustic wave radiation by tessellated transducers with folded curvatures

Danielle T. Lynd, Chengzhe Zou, Joseph Crump and Ryan L. Harne
Mechanical and Aerospace Engineering, The Ohio State University, Columbus, OH, 43210; lynd.47@osu.edu; zou.258@osu.edu; crump.1@themetroschool.org; harne.3@osu.edu

Foldable, origami-inspired transducer arrays have recently been found to offer a straightforward approach of topological transformations on a single tessellated array, rather than signal controls on many transducers, to enable orders of magnitude tuning of acoustic wave guiding capability. Although optimization approaches exist to develop tessellations that serve simple mechanical functions, there are not yet established methods to design tessellated acoustic arrays for targeted acoustic wave guiding properties. This research presents a first approach to design, evaluate, and iteratively refine the tessellations that make up origami-inspired acoustic transducer arrays for desired wave guiding abilities. To exemplify the procedure, two folding patterns are investigated using this process. The approach aims to integrate computational tools to create the tessellation, modify the design based on intuition or prior knowledge, evaluate the acoustic wave radiation characteristics, and iterate on the design according to the outcomes of the evaluations. The two examples exemplify the efficacy of this new process and identify means for improvement and automation. The approach will enable ongoing efforts to devise origami-inspired acoustic transducers and arrays that may serve diverse applications demanding adaptable acoustic wave energy guiding, from biomedical imaging and diagnostics to portable communication and alert devices.

Published by the Acoustical Society of America

 https://doi.org/10.1121/2.0000667

1. INTRODUCTION

The guiding of acoustic energy in real time is important for many applications. Arrays of acoustic transducers are used to determine the sources of noise from jets and rocket engines [1-3] using digital methods that create an acoustic "camera" from numerous microphones fixed in their locations. Focused ultrasonic waves are digitally created, transmitted, and then interpreted upon reflected reception for use in biomedical and industrial imaging [4-7]. Ultrasonic therapy is also used to treat cancer by locally heating the locations where tumors exist, via constructive interference of waves enabled by digitally controlled signal delays to individual array elements [8-10]. For these purposes, phase delays between the activation of the transducers and amplitude weights among transducers are established via digital signal processing approaches to create constructive and destructive interference, allowing for acoustic beams to be directed or focused [5, 11]. On the other hand, digital controls of the signals to realize arbitrarily guided acoustic wave fields come with a set of unique challenges. Arrays that require better focused or more directive sound energy must employ many transducers distributed over large spaces [12], creating a computational burden for real-time control, limiting portability, and increasing complexity of implementation [13].

These problems motivate the exploration of innovative methods of shaping and focusing acoustic energy that are not subject to the same challenges. Seeing a structural analogy between the planar transducers configurations of acoustic arrays with the distributed, periodic tessellations of origami folding patterns, the authors recently explored [14] a concept of origami-inspired acoustic transducer arrays to bypass these challenges to control wave fields.

Indeed, origami has served as an inspiration for numerous recent innovations in the fields of mathematics, architecture, and engineering [15, 16]. The mechanical properties of an origami fold can be tuned through small adjustments to the crease patterns [17, 18], while the tessellated patterns may also inspire deployable structures, which fold to smaller sizes for portability and strategic deployment in difficult to access locations [19-21]. Central to the creation of origami tessellations are periodic patterns of planar facets. These periodic patterns and low-dimensionality of the folding patterns permit large reconfigurability of origami-inspired array structures, including radio frequency antenna [22] and deployable systems [19]. In the recent work, the authors identify the similar compatibility between the periodic facets of tessellations and the traditional fabrication of acoustic transducer arrays [14], although the latter are ordinarily fixed in position and controlled digitally to adapt wave guiding properties.

In the prior efforts, Miura-ori [14] and star-shaped [23] folding patterns were investigated as candidate shape-transforming tessellations upon which acoustic transducers are placed or adhered for uniform driving. By the topological reconfiguration due to simple mechanical or kinematic folding actions, the acoustic wave fields were seen to adapt by orders of magnitude in the near and far field -- i.e. few or many acoustic wavelengths from the array -- without recourse to digital control approaches. These efforts were undertaken using analytical and computational methods, while experimental validations were provided to ground the feasibility of the concept through practical demonstrations.

On the other hand, developing tessellated arrays whose shape transformations provide acoustic wave focusing in the near field or selective angular transmission of acoustic energy far from the array encourages an automated or semi-automated approach for design and evaluation rather than the detailed theoretical treatments applied in [14, 23].

Building upon the recent work, this report describes a set of integrated computational procedures to design new tessellations to be used as foldable, adaptive acoustic transducers and arrays. The following section describes the computational pathway realized to progress from a desired wave field characteristic to the determination of a tessellated transducer or array geometry that meets the aim. Then, two examples are provided and contrasted for their effectiveness at achieving their goals. Summary remarks conclude this report.

2. COMPUTATIONAL TOOL INTEGRATION TO DESIGN FOLDABLE, TESSELLATED ACOUSTIC TRANSDUCERS AND ARRAYS

This research draws together a sequence of computational steps to realize a goal for particular acoustic wave guiding. As depicted in Figure 1, a first step is to develop a tessellation base, either through topology optimizers or through inspiration from existing literature. Then, following modifications to the tessellation, which may be few on a first trial, computer simulations are employed to transform the unfolded pattern into folded construction. Finally, the boundary element method accepts this transformed tessellation shape as topological input, performs required procedures to mesh the tessellation surface and to associate certain surfaces with the active acoustic transducers, and then simulates the acoustic wave field generated by the origami-inspired acoustic transducer array. These steps are explained in greater detail in the following sections.

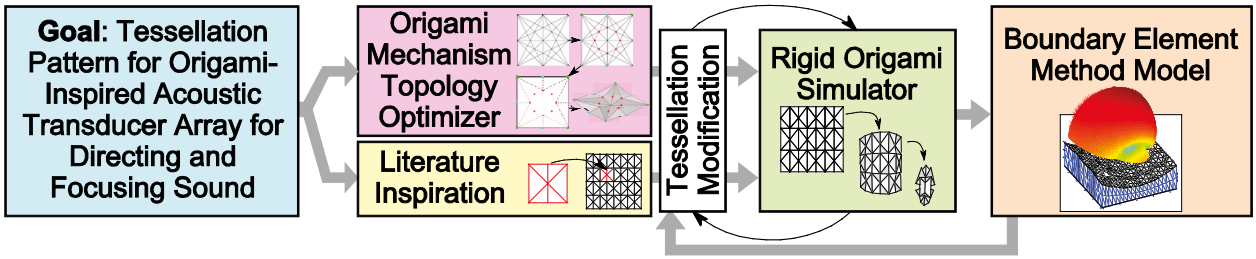

Figure 1. Pathway to proceed from target transducer or array characteristics, through tessellation design, modification, folding simulation, and acoustic modeling.

A. DESIGNING A FOLDABLE TESSELLATION

Central to the creation of foldable, acoustic transducer arrays is the design of tessellations upon which the array can be based. In other words, the tessellations are presumed to be partially or fully occupied by acoustic transducers, so that the folding operations reposition and orient the transducers for adaptive acoustic energy delivery capabilities. Certain characteristics of the tessellations are desired respecting the aims to guide acoustic energy in an adaptive structural framework. (i) Developable, rigid foldable tessellations [24] are preferred to promote the concept of easily manufactured acoustic arrays with readily adapted wave guiding capabilities. Because all flat, planar radiators inherently exhibit angular directionality of acoustic wave delivery to far field points [25], (ii) the shape transformations of the tessellated array should effect curvature that culminates in near field acoustic wave focusing [26], similar in concept to the design of satellites or optical lenses. In so doing, the tessellated array will provide directive acoustic wave radiation when unfolded and adaptively focused wave fields when folded to different extents [23]. In addition, (iii) flat foldable arrays are sought for sake of enhancing portability of the array since it may be compacted when transported or when otherwise not needed, such as a concept for a portable and easily deployable loudspeaker line array [27]. Based on these three design goals, the following Secs. 2.1.1 and 2.1.2 describe computational approaches to firstly devise the initial folding pattern. Sec. 2.2 describes the evaluation of acoustic transducer arrays formulated on such tessellations, the outcomes of which iteratively feed back into the design process, as illustrated in Fig. 1.

i. Literature-inspired tessellations

A straightforward approach to create a tessellation suitable for use as a substrate for an acoustic transducer or array is to take inspiration from the literature and modify the pattern as needed. Indeed, the literature is rich with inspiration for origami tessellations and their derivatives. Evans [28] studies several rigidly foldable tessellations, while Sareh and Guest [29,30] have characterized isomorphic and non-isomorphic adjustments to Miura-ori showing a significant range of folding structures is possible by tailoring the common Miura-ori pattern. Also, Dudte et al. [31] have shown that arbitrary curvatures may be effected using Miura-ori variants. Inspired by these or other works, a tessellation may be selected for investigation as an acoustic transducer or array substrate. Once a folding pattern is selected, it may be modified to meet needs according to informed experience from past studies. One folding pattern adapted from literature to be considered here is the waterbomb, which is shown in Figure 2(a). As used elsewhere throughout this report, red lines on the folding pattern indicate valley folds, while blue lines represent mountain folds. Yet, to

realize an array, the waterbomb constituent of Fig. 2(a) is modified, as shown in Fig. 2(b). This permits assembly of many constituents into the array shown in Fig. 2(c) that effects a cylindrical curvature when folded, Fig. 2(d,e). The inward, cylindrical folded shape intuitively suggests a focal point exists where acoustic waves emitted from the array may constructively interfere for near field focusing.

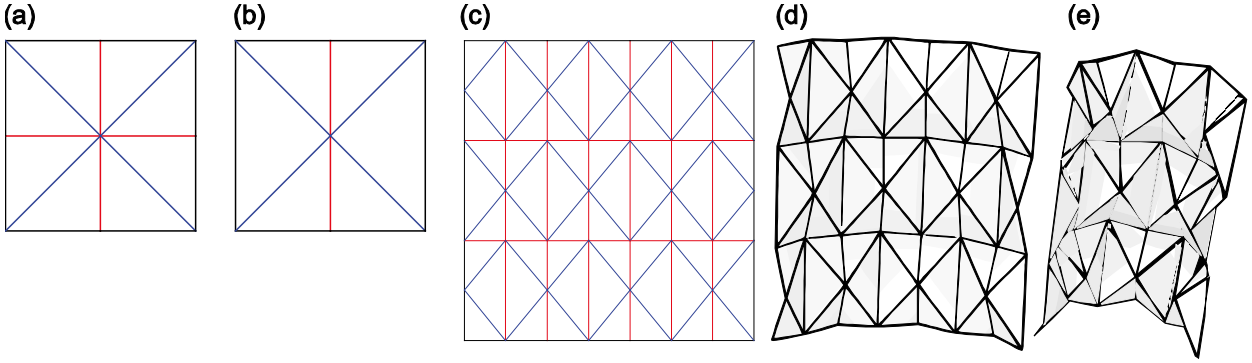

Figure 2. The waterbomb unit cell in (a) is modified to its form in (b), to enable the assembly of the array in (c). Two folding arrangements are depicted in a (d) slightly folded configuration to (e) more folded configuration.

ii. Topology optimization tessellation creation

A computer-aided process may reduce the time it takes to create such a tessellation when compared to extensive literature search for inspiration. Origami topology optimizers provide one such semi-automated process for tessellation design. For instance, Lang [32] developed the TreeMaker software, which utilizes nonlinear constrained optimization to create and explore the folding of origami and tessellations. Fuchi et al. [33] established a topology optimization algorithm, the Origami Mechanism Topology Optimizer (OMTO), to design origami-based mechanisms that meet prescribed boundary conditions and performance metrics when loaded by applied forces. Continued optimizer improvements have led to accurate accounting for geometric and material stiffening for folded tessellated mechanisms [34]. In this research, the OMTO software is utilized to facilitate tessellation design according to the desired characteristics for adaptive, foldable acoustic arrays. Namely, the inward conformations of a transducer suggest opportunity for near field focusing of acoustic waves. Thus, the implementation of OMTO in this study is set to realize inwardly pointing topologies as a tessellation is folded. Readers interested in the detailed workings of OMTO are referred to [33].

One folding pattern created here using OMTO is termed the four-pointed star. Figure 3(a) depicts the four-pointed star folding pattern. Fig. 4(b) shows a modified variant termed the six-pointed star that exhibits greater inward pointing of the facets when the tessellation is folded, seen in Fig. 4(c). Consequently, the folding conformations of the six-pointed star suggest greater potential than the four-pointed star for near field focusing of acoustic waves transmitted from the facet surfaces. In fact, the principles of the star-shaped tessellation may be modified to derive new tessellations. Namely, at the core of the folding pattern is an alternating sequence of mountain and valley folds radially extending from a central node. Manipulation of this pattern, and various assemblies of such constituent into arrays, may realize a breadth of acoustic array architectures, similar to that achieved using the waterbomb constituent in Fig. 2.

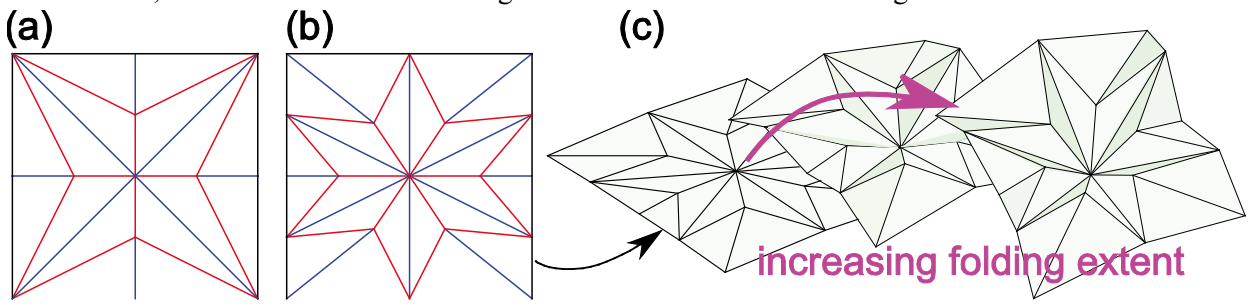

Figure 3. The tessellations of the (a) four-pointed and (b) six-pointed stars. The unfolded, slightly folded, and more folded configurations of the six-pointed star are in (c).

B. RIGID ORIGAMI SIMULATION

Once the folding patterns of tessellation candidates are designed, such as the waterbomb array and the six-pointed star, the shape transformations must be simulated. For rigidly foldable tessellations, Tachi's [35] Rigid Origami Simulator (ROS) is shown to accurately emulate kinematic folding. Importantly for the following step of the developments of this work, the resulting nodes and node-element connectivity of the folded tessellation are available as output from ROS. Thus, in this research, we translate tessellations inspired from literature or developed from topology optimizers, and potentially modified, into ROS for folding to prescribed extents. The waterbomb array shown in Fig. 2(d,e) and six-pointed star shown in Fig. 3(c) are illustrated in folded configurations realized using ROS. The transformed topology information of nodes and element connectivity is then leveraged for subsequent acoustic modeling.

C. ACOUSTIC WAVE PROPAGATION MODELING BY THE BOUNDARY ELEMENT METHOD

Once the tessellations are designed, modified, and then folded in simulation, in this research all of the tessellated surfaces are presumed to oscillate with time-harmonic, constant surface normal velocity. This is effectively realized in the corresponding experimental components of this work in which case acoustic transducers cover part or all of the tessellation surfaces and are driven in parallel [14,23]. In this way, the devised tessellations radiate sound with wave field characteristics adapted according to the shape reconfigurations realized by folding, according to the development of constructive and destructive interferences in the field. For such assessments in acoustics applications, the boundary element method (BEM) is used to solve the Helmholtz integral equation to determine the sound pressure level (SPL) at locations in the free acoustic field. Completing the direct, forward process of tessellation and evaluation by the flowchart of Fig. 1, here the openBEM software [36] is implemented to characterize the radiated acoustic fields from the foldable tessellations. The mesh is generated via a MATLAB script that bounds the tessellation in an effective baffle as shown in Fig. 1 at right, where the tessellation mesh is shown with black lines while the bounding box mesh is shown with blue lines. A representative simulation result is shown over top of the tessellated array in Fig. 1 at right, similar to the locations of acoustic wave evaluation of interest here. Due to requirements for accuracy in BEM simulations, all results reported hereafter use at least 6 elements per acoustic wavelength.

Once evaluated, trends observed can help to inform changes to the tessellated transducer or array folding patterns, as shown via the feedback loop of Fig. 1. Indeed, once even preliminary information is available from BEM simulations, the modifications to the tessellations may not necessarily require BEM evaluation on each iteration to test the new shape transformations of folding sequences via ROS. Due to the computational challenges of BEM, such iteration without BEM simulation on each evaluation may be preferred.

3. RESULTS AND DISCUSSIONS

By drawing inspiration from literature, utilizing topology optimization software, and after further modifications to the tessellation to comply with basic understanding of acoustic wave propagation phenomenon, two foldable acoustic wave radiators are created in this study for close consideration. The first is the waterbomb acoustic transducer array shown in Fig. 2(c,d,e), which is established upon a modified version of the waterbomb base constituent, shown in Fig. 2(a) in original and 2(b) in modified forms. The second wave radiator considered is the six-pointed star acoustic transducer constituent, shown in Fig. 3(b,c) that may be assembled into arrays.

The following sections assess the effectiveness of the two foldable acoustic transducers and arrays to guide wave energy to points in the near and far field via folding sequences, thus meeting the goal for which they are designed.

A. WATERBOMB ACOUSTIC TRANSDUCER ARRAY

BEM simulation results of the sound pressure level (SPL), presented in dB with a 20 μPa reference, are shown in Figure 4 when the waterbomb array is slightly folded and driven with a frequency of 3 kHz. The

plot shows the SPL in a spherical coordinate system with angular position (β,ϕ) where β is the elevation angle and ϕ is the azimuthal angle. For a given combination of (β,ϕ), the radial distance from the origin is the SPL evaluated at that angular location for the prescribed radial distance R provided in the figure. The color of the surface is similarly shaded to denote the SPL. As a result, the common radial distance evaluation helps one to understand the effectiveness of wave energy delivery across a common radial range for a variety of angular regions. This plotting method is conventional in the assessment of three-dimensional wave propagation from acoustic arrays [37] and radio frequency antenna [38], and helps to visualize the "strength of emission" from the origin where the array is positioned, as illustrated in the parts of Fig. 4. This visualization technique also means that each axis of Fig. 4 is SPL, so that the magnitude of a given surface location from the origin at a combination of (β,ϕ) denotes the SPL at that angular position (β,ϕ) in the field.

The waterbomb array is assembled from constituents with largest side length of 25 mm. From Fig. 4(a) to (b) to (c), the radial location R in the acoustic field from the center of the unfolded tessellation changes from 19.4 mm to 125 mm to 625 mm, respectively. Effectively, these represent hemispheres that are each progressively further from the transducer array. Based on the constituent characteristic length and folding extent, the geometric (and acoustic) focal point of the foldable array is around 100 mm. The radial location of 625 mm lies in the acoustic far field, yet close to the transition distance [5] for reasonable comparison to SPL within the near field.

As shown comparing the "broadside" SPL between Fig. 4(a) and (b), there is an increase around 6 dB of acoustic energy delivered along the central axis. This indicates the focusing abilities of this array, because spherical wave spreading ordinarily diminishes acoustic pressure amplitude by 6 dB for every doubling of distance from the spherical wave source. In other words, despite being more than 4 times more distant from the array, from Fig. 4(a) to (b), rather than experience a 12 dB *reduction* in broadside SPL, the waterbomb acoustic transducer array realizes a 6 dB *gain*, exemplifying the acoustic energy focusing capabilities effected without recourse to digital control approaches. Folding also influences the wave radiation patterns dependent upon the angular location of the field point. The area of low SPL, also called a node, at the radial distance of 125 mm appears approximately at angles around 50-60° from the normal aligned with broadside, whereas a more diffused sound field is observed closer to the array at 19.4 mm since no such nodes occur.

In the far field at a radial range R =625 mm, Fig. 4(c), the broadside SPL reduces to 87 dB whereas the depth of the node is greatly diminished. This indicates that folding the waterbomb array provides acoustic focusing not evident for unfolded, planar radiators of acoustic waves [26] while the same folding process that results in curvature reduces far field directional delivery of wave energy, a well-documented feature of planar radiators [5].

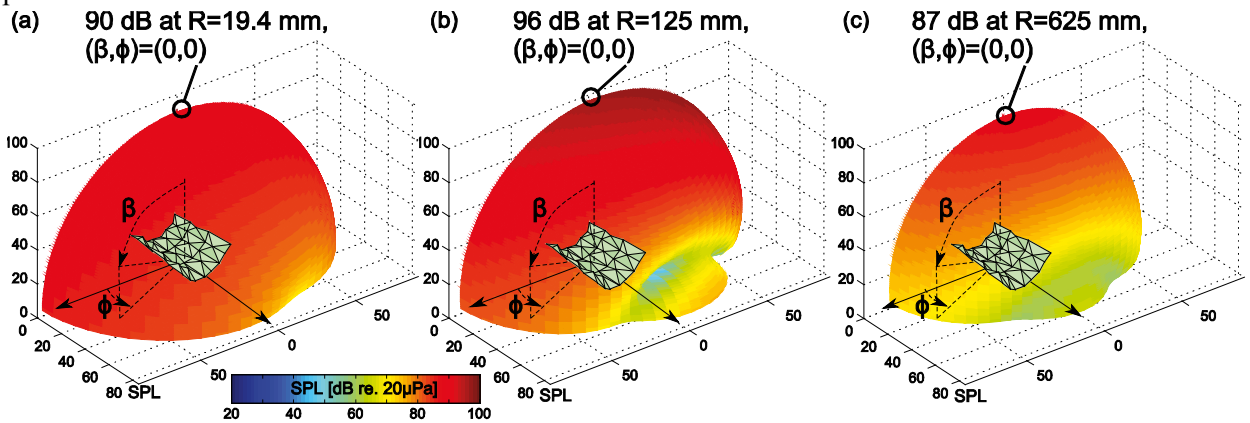

Figure 4. BEM simulation results of SPL at (a) 19.4 mm, (b) 125 mm, and (c) 625 mm from the transducer center point when unfolded. A spherical coordinate system is used to present the SPL from the origin (0,0,0) [dB], such that any given angular location from the origin shows the color and corresponding radial range as the SPL value determined at that angular location. Circle labels emphasize the SPL at broadside and show a relative focusing due to the curvature of the tessellated transducer.

B. SIX-POINTED STAR ACOUSTIC TRANSDUCER CONSTITUENT

The modification of the six-pointed star constituent, from the four-pointed variant, is intended to better promote near field wave focusing phenomenon via a greater proportion of inward pointing facets that provide a convergent wave field to a focal location. Yet, it is also observed that the waterbomb constituent, Fig. 2(a), exhibits inward directed facets when partially folded. Thus, here a comparison is made between the acoustic energy focusing abilities of the unmodified waterbomb constituent, Fig. 2(a), and the six-pointed star constituent, Fig. 3(b), when serving as the substrate for a shape-adaptive acoustic wave radiator.

Figure 5 provides a comparison of BEM simulation results for the broadside SPL emitted by the waterbomb and six-pointed star acoustic transducer constituents. Both constituents have a characteristic side length dimension of 47 mm. The waterbomb transducer is thus square when unfolded. Because the six-pointed star is not square when unfolded, there is a greater surface area of wave radiation for the six-pointed star transducer than for the waterbomb. Fig. 5(a,b,c) show the BEM simulation results for the waterbomb, while Fig. 5(d,e,f) are the results for the six-pointed star. Fig. 5(a,d) shows the simulation results for wave radiation at 5 kHz. The findings reveal that no focusing occurs as the radial distance of evaluation is increased from the transducers, regardless of the folding extents. The folding extents are shown as inset images in the figures. Instead, both tessellated transducers exhibit the anticipated reduction of SPL of approximately 6 dB for every doubling of distance.

Yet, at the frequency 10 kHz, the waterbomb in Fig. 5(b) begins to show signs of focusing, since all three folding extents reveal a peak SPL at broadside around or less than a radial distance of 100 mm from the transducer center. Likewise, at the location nearest to the transducer, the six-pointed star constituent exhibits near field focusing at 10 kHz, in Fig. 5(e), that is induced by folding. Specifically, the unfolded configuration results in about 2 dB less broadside SPL at a radial distance of 10 mm than the most folded configuration. While a small amplification of the SPL, it is evidence of a trend towards acoustic wave focusing sought from the design process. Finally, Fig. 5(c,f) show that at 20 kHz both tessellated transducers provide near field focusing. Yet, the star in Fig. 5(f) shows only about 9 dB of SPL adaptation around a radial distance of 10 mm by folding, whereas the waterbomb may change the SPL by almost 15 dB at 20 mm by transitioning from moderately to significantly folded configurations.

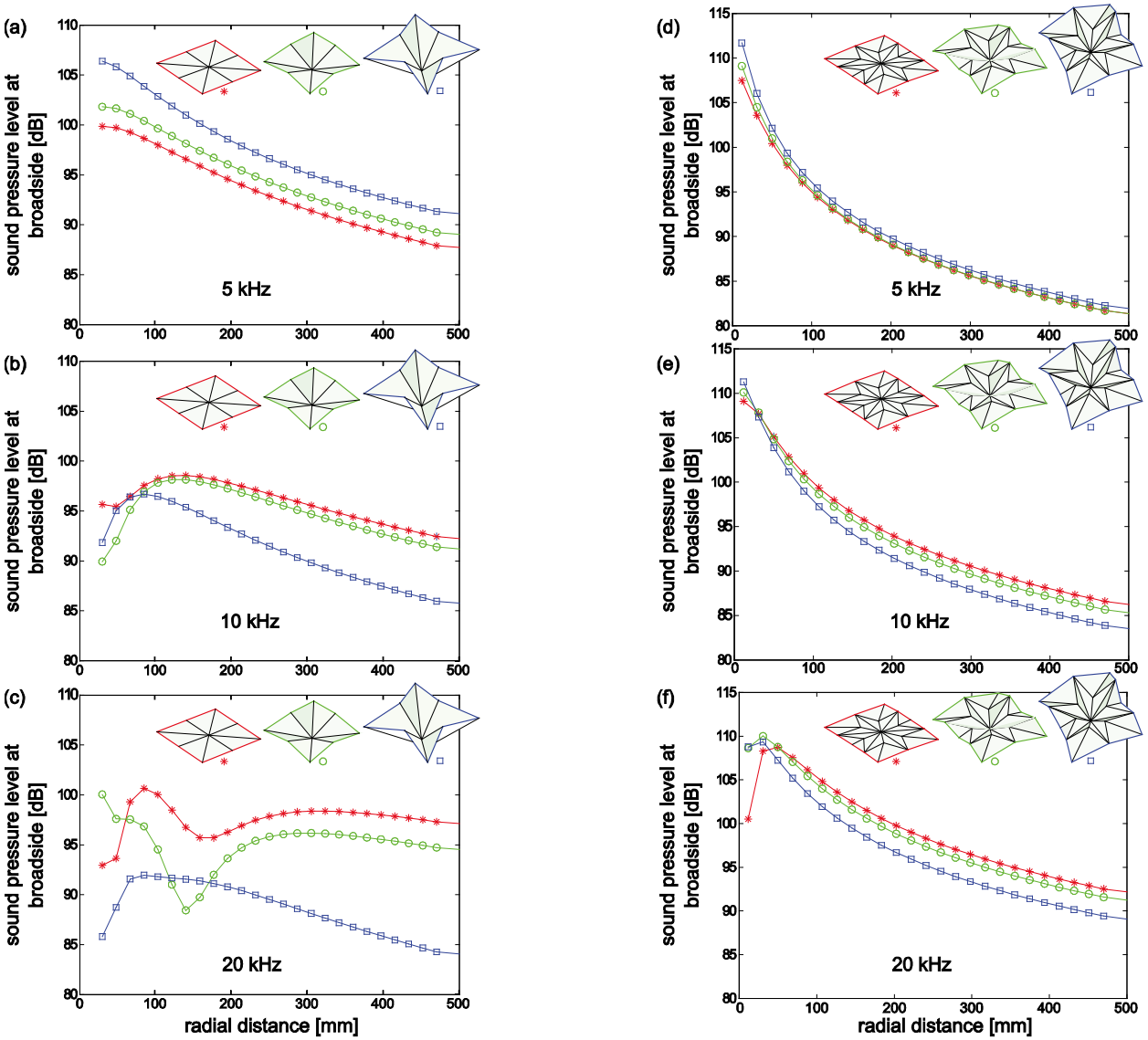

Figure 5. Broadside SPL of waterbomb and six-pointed star acoustic transducer constituents. Results are shown, respectively, for the waterbomb and six-pointed star at (a) and (d) for 5 kHz, at (b) and (e) for 10 kHz, and at (c) and (f) for 20 kHz. BEM simulation results shown for three different folding extents, with corresponding inset images of the folding extents.

These findings demonstrate the interplay between acoustic and structural characteristic dimensions, i.e. the wavelength and transducer geometries. While both transducer constituents of Fig. 5 exhibit inward pointing conformations when folded, an intuition regarding conventional geometric lensing may be misled without the appropriate design and acoustic modeling tools. For instance, the six-pointed star is derived as a variant of the star-shaped tessellation so as to increase the number of facets providing an inward pointing conformation, yet it does not culminate in as great acoustic wave focusing as the waterbomb which is not especially modified for focusing beyond its base folding pattern. Indeed, all of the waterbomb facets point inward when folded. This contrasts with the six-pointed star that has facets that fold in such a way as to point outward, or in a divergent manner away from a conventional geometric focal point. These facets, considered to be radiating acoustic waves, destructively interfere with the ability of the transducer to significantly increase SPL at broadside for the folded configurations. Therefore, iteration of the design, according to the flowchart of Fig. 1 and especially by automated methods, may devise more appropriate ways in which to leverage the star-shaped tessellations for foldable acoustic transducers, including de-activating the outward pointing facets. This exemplifies the need for a computational approach, similar to

that presented in this work, to help a designer find a way to meet the demands of an acoustic wave guiding application with multiple needs within the range of a single foldable, tessellated transducer or array that delivers the combination of requirements though several folded conformations.

Using the computational tools newly integrated in this research, such iteration and re-evaluation of the acoustic energy delivery from the tessellated transducers and transducer arrays is made possible for continued and future explorations. On the other hand, automation of the iterative evaluation and tessellation updating is a task for future work due to the computational burden of excessive BEM evaluations. As such, it is envisioned that optimization approaches, such as gradient-based schemes rather than brute force methods like genetic algorithms, may facilitate the identification of locally or globally optimal tessellations that effect the desired acoustic near and far fields according to their folding extents.

4. CONCLUSIONS

This research establishes an integrated and iterative computational design process to create foldable, tessellated acoustic transducers and arrays for adaptive, real-time acoustic energy delivery to points near and far from the transducer surfaces. This concept bypass challenges of traditional digital control of fixed-location acoustic arrays by leveraging the ordered shape transformations of the tessellations for repeatable shape transformations that provide the needed tuning of interference phenomena for acoustic wave guiding. By literature inspiration or topology optimization, the tessellations may be formulated and then modified according to simulation of their kinematic fold sequences. Once suitably folded, the tessellated transducers and arrays are evaluated by the boundary element method simulation approach. While potentially time-consuming for large acoustic arrays, the BEM modeling enables the investigation of arbitrarily shaped and folded acoustic wave radiators, making it well suited to study the foldable tessellated architectures. The examples presented in this study show that geometric design intuition does not necessarily guide one to immediately achieve acoustic wave focusing using the tessellated structure and folding reconfiguration of the origami-inspired transducers. This may be explained by the fact that the combination of inward and outward pointing facets may compete in the development of the acoustic near field, and may reduce the focusing effects. Further research may explore ways to automate the iterative procedure of evaluation and tessellation modification for computer-assisted design of foldable, tessellated arrays that deliver prescribed acoustic wave energies to arbitrary points in the field.

ACKNOWLEDGMENTS

The authors thank Dr. Kazuko Fuchi of the University of Dayton Research Institute and Drs. Phil Buskohl, Greg Reich, and James Joo of the Air Force Research Laboratory for helpful conversations in regards to the use of the Origami Mechanism Topology Optimizer software. R.L.H. acknowledges start-up funds from the Department of Mechanical and Aerospace Engineering at The Ohio State University. D.T.L. acknowledges support from the Acoustical Society of America via the 2016 Robert W. Young Award for Undergraduate Student Research in Acoustics and from the OSU College of Engineering Honors Research Scholarship. J.C. acknowledges support from The Metro School Research Internship Program.

REFERENCES

1 B.M. Harker, K.L. Gee, T.B. Neilsen, A.T. Wall and M.M. James, "Phased-array measurements of full-scale military jet noise." in *Proceedings of the 20th AIAA/CEAS Aeroacoustics Conference* , (2014), Atlanta, GA, AIAA 2014-3069.

2 D.G. Simons, M. Snellen, B. van Midden, M. Arntzen and D.H.T. Bergmans, "Assessment of noise level variations of aircraft flyovers using acoustic arrays," Journal of Aircraft **52**, 1625-1633 (2015).

3 J. Panda, R.N. Mosher and B.J. Porter, "Noise source identification during rocket engine test firings and a rocket launch," Journal of Spacecraft and Rockets **51**, 1761-1772 (2014).

4 M. Fink, G. Montaldo and M. Tanter, "Time-reversal acoustics in biomedical engineering," Annual Reviews of Biomedical Engineering **5**, 465-497 (2003).

5 M. Postema, *Fundamentals of Medical Ultrasonics* (Spon Press, New York, 2011).

6 F.S. Foster and J.W. Hunt. *The focussing of ultrasound beams through human tissue*. In A.F. Metherell, editor. Acoustical Imaging. (New York: Plenum Press); 1980. 709-718.

7 B.W. Drinkwater and P.D. Wilcox, "Ultrasonic arrays for non-destructive evaluation: a review," NDT&E International **39**, 525-541 (2006).

8 C.C. Coussios, C.H. Farny, G. Ter Haar and R.A. Roy, "Role of acoustic cavitation in the delivery and monitoring of cancer treatment by high-intensity focused ultrasound (HIFU)," International Journal of Hyperthermia **23**, 105-120 (2007).

9 R.E. Beard, R.L. Magin, L.A. Frizzell and C.A. Cain, "An annular focus ultrasonic lens for local hyperthermia treatment of small tumors," Ultrasound in Medicine and Biology **8**, 177-184 (1982).

10 J.Y. Chapelon, D. Cathignol, C. Cain, E. Ebbini, J.U. Kluiwstra, O.A. Sapozhnikov, G. Fleury, R. Berriet, L. Chupin and J.L. Guey, "New piezoelectric transducers for therapeutic ultrasound," Ultrasound in Medicine and Biology **26**, 153-159 (2000).

11 A. Marzo, S.A. Seah, B.W. Drinkwater, D.R. Sahoo, B. Long and S. Subramanian, "Holographic acoustic elements for manipulation of levitated objects," Nature Communications **6**, 8661 (2015).

12 S.C. Wooh and Y. Shu, "Influence of phased array element size on beam steering behavior," Ultrasonics **36**, 737-749 (1998).

13 J.A. Jensen, S.I. Nikolov, K.L. Gammelmark and M.H. Pedersen, "Synthetic aperture ultrasound imaging," Ultrasonics **44**, e5-e15 (2006).

14 R.L. Harne and D.T. Lynd, "Origami acoustics: using principles of folding structural acoustics for simple and large focusing of sound energy," Smart Materials and Structures **25**, 085031 (2016).

15 P. Wang-Iverson, R.J. Lang and M. Yim, editors, *Origami 5: Fifth International Meeting of Origami Science, Mathematics, and Education* (CRC Press, Boca Raton, 2011).

16 K. Fuchi, P.R. Buskohl, G. Bazzan, M.F. Durstock, G.W. Reich, R.A. Vaia and J.J. Joo, "Design optimization challenges of origami-based mechanisms with sequenced folding," Journal of Mechanisms and Robotics **8**, 051011 (2016).

17 J.L. Silverberg, A.A. Evans, L. McLeod, R.C. Hayward, T. Hull, C.D. Santangelo and I. Cohen, "Using origami design principles to fold reprogrammable mechanical metamaterials," Science **345**, 647-650 (2014).

18 A.A. Evans, J.L. Silverberg and C.D. Santangelo, "Lattice mechanics of origami tessellations," Physical Review E **92**, 013205 (2015).

19 S.A. Zirbel, R.J. Lang, M.W. Thomson, D.A. Sigel, P.E. Walkemeyer, B.P. Trease, S.P. Magleby and L.L. Howell, "Accommodating thickness in origami-based deployable arrays," Journal of Mechanical Design **135**, 111005 (2013).

20 T.A. Evans, R.J. Lang, S.P. Magleby and L.L. Howell, "Rigidly foldable origami gadgets and tessellations," Royal Society Open Science **2**, 150067 (2015).

21 Y. Chen, R. Peng and Z. You, "Origami of thick panels," Science **349**, 396-400 (2015).

22 K. Fuchi, A.R. Diaz, E.J. Rothwell, R.O. Ouedraogo and J. Tang, "An origami tunable metamaterial," Journal of Applied Physics **111**, 084905 (2012).

23 C. Zou and R.L. Harne, "Adaptive acoustic energy delivery to near and far fields using foldable, tessellated star transducers," Smart Materials and Structures **26**, 055021 (2017).

24 T. Tachi, "Geometric considerations for the design of rigid origami structures." in *Proceedings of the International Association for Shell and Spatial Structures)IASS) Symposium 2010*, (2010), Shanghai, China, 1-12.

25 L.E. Kinsler, A.R. Frey, A.B. Coppens and J.V. Sanders, *Fundamentals of Acoustics* (John Wiley and Sons, New York, 2000).

26 H.T. O'Neil, "Theory of focusing radiators," The Journal of the Acoustical Society of America **21**, 516-526 (1949).

27 M.S. Ureda, "Analysis of loudspeaker line arrays," Journal of the Audio Engineering Society **52**, 467-495 (2004).

28 T.A. Evans, "Deployable and foldable arrays of spatial mechanisms," (Brigham Young University, Salt Lake City, Utah, USA, 2015). Report No.: Master's thesis.

29 P. Sareh and S.D. Guest, "Design of non-isomorphic symmetric descendants of the Miura-ori," Smart Materials and Structures **24**, 085002 (2015).

30 P. Sareh and S.D. Guest, "Design of isomorphic symmetric descendants of the Miura-ori," Smart Materials and Structures **24**, 085001 (2015).

31 L.H. Dudte, E. Vouga, T. Tachi and L. Mahadevan, "Programming curvature using origami tessellations," Nature Materials **15**, 583-588 (2016).

32 R.J. Lang, "A computational algorithm for origami design." in *Proceedings of the Twelfth Annual Symposium on Computational Geometry*, (1996), Philadelphia, Pennsylvania, USA, 98-105.

33 K. Fuchi, P.R. Buskohl, G. Bazzan, M.F. Durstock, G.W. Reich, R.A. Vaia and J.J. Joo, "Origami actuator design and networking through crease topology optimization," Journal of Mechanical Design **137**, 091401 (2015).

34 M. Kuhn, K. Fuchi, G. Bazzan, M.J. Durstock, J.J. Joo, G.W. Reich, R.A. Vaia and P.R. Buskohl, "Coupling of geometric and material stiffening mechanisms in origami design." in *Proceedings of the ASME 2016 International Design Engineering Technical Conferences and Computers and Information in Engineering Conference*, (2016), Charlotte, North Carolina, USA, DETC2016-60132.

35 T. Tachi. *Simulation of rigid origami*. In Origami 4, Fourth International Meeting of Origami Science, Mathematics, and Education. (Natick, Massachusetts: A K Peters, Ltd.); 2009. 175-188.

36 V.C. Henriquez and P.M. Juhl, "OpenBEM - an open source boundary element method software in acoustics." in *Proceedings of Internoise 2010*, (2010), Lisbon, Portugal, 1-10.

37 E.G. Williams, *Fourier Acoustics: Sound Radiation and Nearfield Acoustical Holography* (Academic Press, San Diego, 1999).

38 H.J. Visser, *Array and Phased Array Antenna Basics* (John Wiley & Sons Ltd., Chichester, 2005).